Materials Science-Poland, Vol. 23, No. 1, 2005

The sol-gel synthesis of bismuth titanate electroceramic thin films

ALDONA ZARYCKA*, AGATA LISIŃSKA-CZEKAJ, JUSTYNA CZUBER,
TOMASZ ORKISZ, JAN ILCZUK, DIONIZY CZEKAJ

University of Silesia, Department of Materials Science, ul. Śnieżna 2, 41-200 Sosnowiec, Poland

The present study reports results of the synthesis of randomly oriented $Bi_4Ti_3O_{12}$ (BTO) thin films by a modified hybrid sol-gel process. Bismuth nitrate and titanium(IV) butoxide were used as the starting materials. Crystalline films were deposited on silicon and stainless steel substrates by spin coating and subsequently annealed at 650 °C. The structure of the films was investigated by X-ray diffraction. The formation of a layered perovskite-like structure with orthorhombic symmetry was confirmed. Scanning electron microscopy showed that the surfaces of the films were smooth, dense, and crack free. Conservation of the chemical composition was confirmed by energy dispersive spectroscopy.

Key words: $Bi_4Ti_3O_{12}$; ferroelectric thin films; sol-gel method; X-ray studies

1. Introduction

In recent years, considerable attention has been devoted to the development of thin film technologies for perovskitic materials due to their technically important properties [1]. Depending on the stoichiometry used, such materials exhibit ferro-, piezo- and pyroelectric, or electrostrictive properties. Their composition can also be adjusted to attain electronically conductive materials.

We will concentrate on thin films of materials from the Aurivillius family. Attention to the Aurivillius phases, which constitute a wide family of layered compounds, has increased due to their potential use in electrooptic devices. They are generically described as intergrowth structures of fluorite-like $(Bi_2O_2)^{2+}$ units and perovskite-like $(A_{n-1}B_nO_{3n+1})^{2-}$ slabs, where n = 1–5 or 8 [2]. The 12-fold perovskite A sites can be occupied by mono-, di-, or trivalent cations like Na^+ Ba^{2+}, Ca^{2+}, Sr^{2+}, Bi^{3+}, and rare-earth cations. The 6-fold B sites are usually occupied by smaller cations like Ti^{4+}, Ta^{5+}, Nb^{5+}, and W^{6+}, leading to BO_6 octahedra [3].

*Corresponding author, e-mail: azarycka@us.edu.pl.

Bismuth titanate $Bi_4Ti_3O_{12}$ (BTO) was synthesized by Aurivillius in 1949 [4]. Due to its structural characteristics, BTO single crystals are strongly anisotropic in terms of ferroelectric properties such as polarization and coercive field. The polarization direction of BIT is 4.50 of its cell structure base plane, thus giving rise to a much larger *a*-axis polarization (P_s = 45–50 μC/cm^2) than *c*-axis polarization (P_s = 4.5 μC/cm^2) [5]. If bismuth-layered perovskite films are to be used in ferroelectric thin film capacitors with plane electrodes on the top and bottom (as in the geometry used for dynamic random access memories), however, a polarization component oriented normally to the electrode plane is essential. The preparation of randomly oriented thin films of this family has thus become a challenging issue, since the anisotropy phenomenon is expected to be critical for high-density devices [6]. Therefore, we concentrate on the growth of randomly oriented BTO thin films in the present study.

The idealized structure (space group (SG) *I*4/*mmm*; $a_T \approx 3.86$ A and $c_T \approx 32.8$A) of the $n = 3$ Aurivillius compound $Bi_4Ti_3O_{12}$ is shown in Fig. 1.

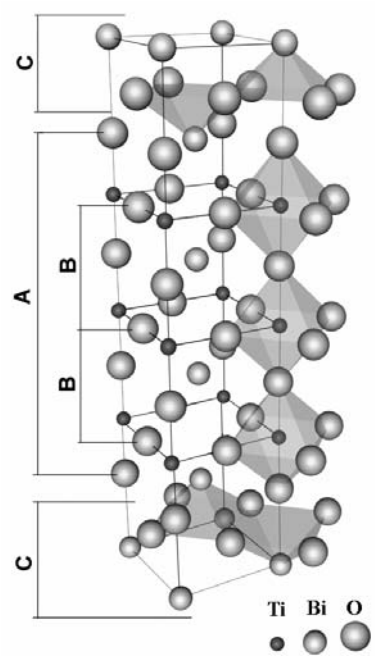

Fig. 1. Half of the pseudotetragonal unit cell of $Bi_4Ti_3O_{12}$ (for z = 0.25–0.75): A – the perovskite layer $Bi_2Ti_3O_{12}^{2-}$, C – the $Bi_2O_2^{2+}$ layers, B – the unit cell of the hypothetical perovskite structure $BiTiO_2$ (after [4])

Quite different chemical and physical methods have been used to deposit $Bi_4Ti_3O_{12}$ thin films, e.g., RF sputtering, sol-gel processing, laser ablation, and metal-organic chemical vapour deposition [7]. These methods are competitive and each of them has advantages and disadvantages in terms of homogeneity, processing temperatures, and processing costs.

Processing high-quality thin films requires low-temperature synthesis, high reproducibility, simplicity in all processing steps, and low cost. Due to these requirements, the search for new routes of films preparation remains an interesting and open subject,

in order to improve the stability of complex solutions, enhance stoichiometry control in film composition, or reduce the cost of the process.

In the presented research, we succeeded, using a hybrid sol-gel spin coating method, in growing randomly oriented $Bi_4Ti_3O_{12}$ thin films on silicon and stainless steel substrates. Their microstructures, structures, and chemical compositions were studied.

2. Experimental

A modified sol-gel process was employed to prepare $Bi_4Ti_3O_{12}$ thin films. Bismuth nitrate $Bi(NO_3)\times 5H_2O$, instead of bismuth acetate, and titanium(IV) butoxide $Ti(OC_4H_9)_4$ were used as the starting materials [8]. Bismuth nitrate was dissolved in 2-methoxyethanol to form bismuth solution, while titanium(IV) butoxide was stabilized by acetyloacetone to form titanium solution. An excess of 10% Bi was used to compensate the evaporation of bismuth during annealing. $Bi_4Ti_3O_{12}$ precursor solution was then obtained by mixing the two solutions. After that deionised water was added to this mixture while stirring. The advantage of using 2-methoxyethanol as the solvent of bismuth nitrate in the present study (over the generally used acetic acid) is that it dissolves bismuth nitrate at room temperature. After thorough mixing, the precursor solution was used to deposit $Bi_4Ti_3O_{12}$ thin films on silicon, glass, and stainless steel substrates by spin coating at 3500 rpm for 30 s.

Amorphous films were kept in a preheated furnace at 350 ºC for 5 minutes to remove the volatile organic components. The coating process (i.e., spinning – drying – pyrolysis) was repeated up to 10 times. The as-deposited films were then heat-treated at 650 °C for 2 hours to form a good crystal structure [9].

The crystalline structures of the annealed thin films were examined by X-ray diffraction (XRD) analysis, using a Philips PW 3710 X-ray diffractometer with Co$K_{\alpha 1\alpha 2}$ radiation. Scanning electron microscopy (HITACHI S-4700-type microscope) was used to study the surface morphology of the films. The stoichiometry of the films was investigated using a chemical composition analysis system (EDS) of the VANTAGE type. All characterizations were carried out at room temperature.

3. Results and discussion

The surface morphologies of the thin films grown on stainless steel and silicon substrates are given in Fig. 2. Although the temperature of crystallization of the BTO thin films was the same for both types of substrates (T = 650 °C for 2h), one can see influence of the substrate on the crystallization conditions. We can conclude, however, that our modified sol-gel technique can prevent the formation of cracks and yields homogeneous dense nanocrystaline microstructures, similar to those arising from films prepared by the sol-gel technique elsewhere [10, 11].

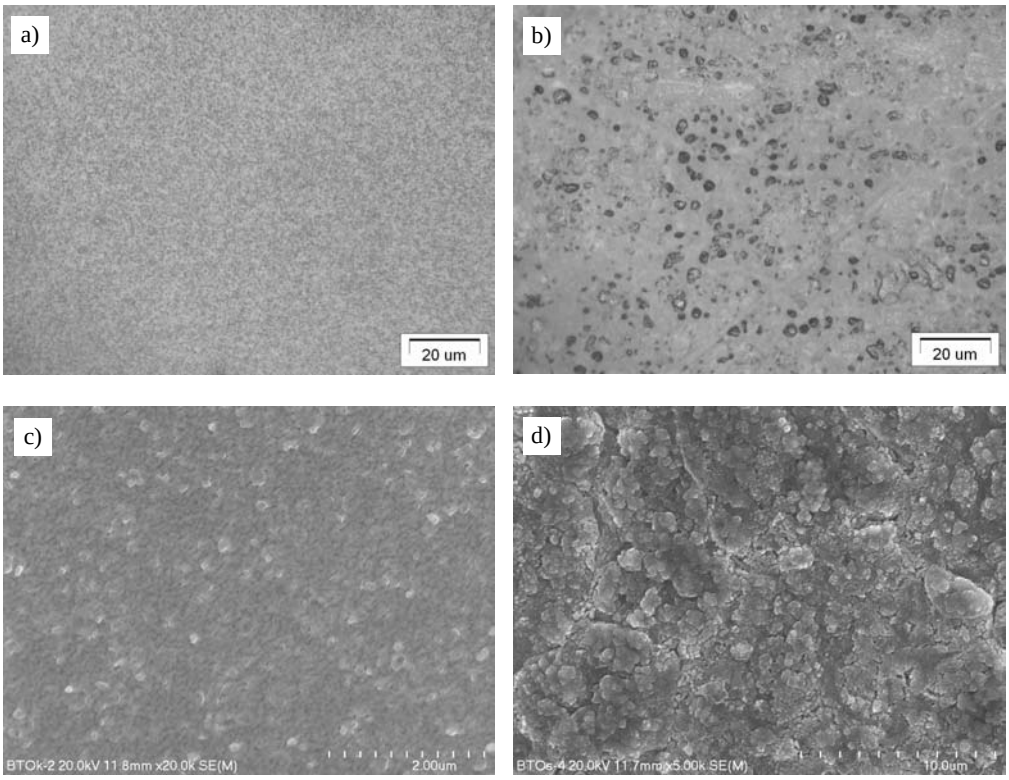

Fig. 2. Optical (a, b) and SEM images (c, d) of the surfaces of BTO thin films deposited on silicon substrates (a, c) and stainless steel substrates (b, d)

Point analysis of the chemical composition in micro–areas for BTO on stainless steel substrates was done by EDS. The results of these measurements give the following compositions of the thin films: Ti – 11.70 wt. %, Bi – 72.20 wt. %, O – 16.10 wt. %. On the other hand, the results of theoretical calculations for stoichiometric $Bi_4Ti_3O_{12}$ give: Ti – 12.26 wt. %, Bi – 71.35 wt. %, O – 16.39 wt. %.

The actual crystal structure of BTO was determined by Rae et al. [12] from single -crystal XRD data. It was described as a commensurate modulation of an orthorhombic average structure (SG *Fmmm* No. 69; $a_{orth} \approx b_{orth} \approx a_{tet}\sqrt{2}$ and $c_{orth} = c_{tet}$) that leads to a monoclinic system (SG *B*1*a*1 No. 7, non-standard setting of *P*1*c*1) with a_{mon} = 5:450(1)Å, b_{mon} = 5.4059(6)Å, c_{mon} = 32.832(3)Å, and β = 90.00° (the non-conventional B cantering is used for easy comparison with the parent *I*4/*mmm* prototype and the *a*- and *b*-axis corresponding to the diagonals $a_{tet} \pm b_{tet}$ of the parent structure) [13].

The XRD patterns of the produced BTO films revealed that good crystalline $Bi_4Ti_3O_{12}$ films were obtained (Figs. 3, 4). Careful examination of the XRD patterns indicates that there is no preferred orientation for any sample. The lattice parameters for $Bi_4Ti_3O_{12}$ were calculated for the orthorhombic phase of bismuth titanate using the Rietveld refinement [14] built into the computer program PowderCell 2.4 [15].

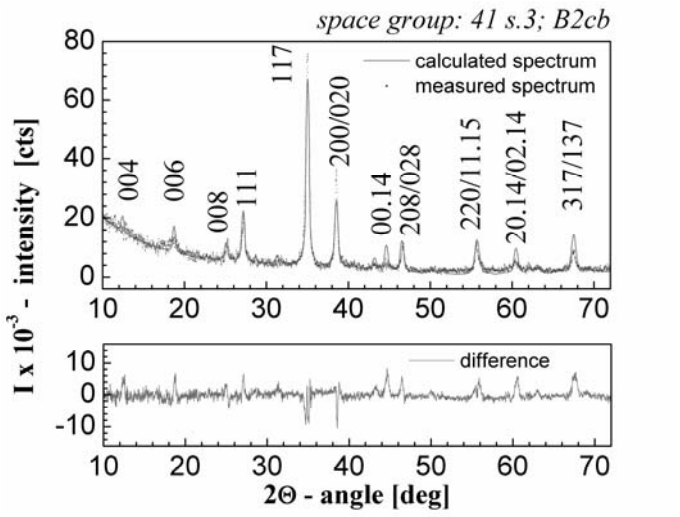

Fig. 3. Results of X-ray pattern fitting for BTO thin films on silicon substrates (circles – raw data points, the solid line – the best calculated profile according to the *B*2*cb* space group). The trace at the bottom is a plot of the difference between the calculated and observed intensities

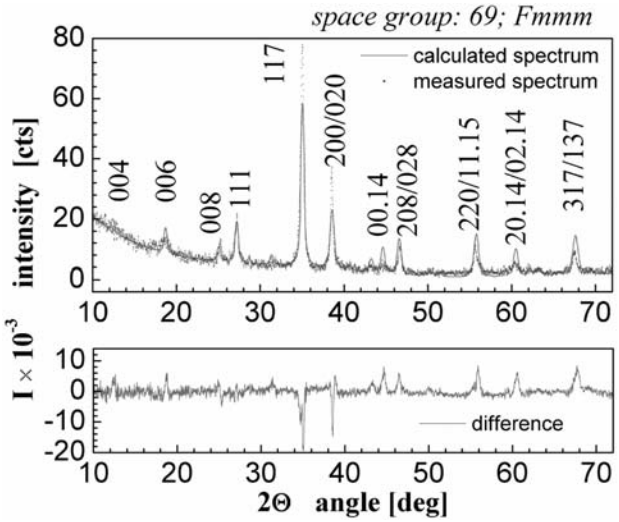

Fig. 4. Results of X-ray pattern fitting for the BTO thin film on silicon substrates (circles – the observed pattern, solid line – the calculated pattern according to the *Fmmm* space group). The trace at the bottom is a plot of the difference between the calculated and observed intensities

Two model structures were used, both of the orthorhombic symmetry, namely *B*2*cb* (ICSD, data file No. 16488 [16]) (Fig. 3), and *Fmmm* (ICSD, data file No, 24735 [4]) (Fig. 4). Detailed information about the model structures is given in Tables 1 and 2, whereas the details of the calculated X-ray spectra are given in Tables 3 and 4.

Table 1. Parameters of the model structure used for XRD pattern fitting (see Fig.3)

Space group number	41
Space group	*B*2*cb*
Cell choice	3
Lattice parameters	5.4162 Å, 5.4132 Å, 32.9200 Å
Angles	90.00°, 90.00°, 90.00°,
Atoms in asymmetric unit	10
Atoms in unit cell	76.0, 76 generated position
Volume of cell	965.18 $Å^3$
Relative mass of unit cell	4686.47
X-ray density	8.0628 g/cm^3
Mass absorption coefficient	287.41 cm^{-1}/g

Name	P. No.	Ion	Wyck.	*x*	*y*	*z*	SOF	*B*
Bi1	83	Bi^{3+}	8b	0.0000	0.9978	0.0668	1.00	1.00
Bi2	83	Bi^{3+}	8b	0.9991	0.0199	0.2113	1.00	1.00
Ti1	22	Ti^{4+}	4a	0.5452	0.0000	0.0000	1.00	1.00
Ti2	22	Ti^{4+}	8b	0.0533	0.9990	0.3714	1.00	1.00
O1	8	O^{2-}	8b	0.2070	0.2220	0.9967	1.00	1.00
O2	8	O^{2-}	8b	0.2640	0.2520	0.2507	1.00	1.00
O3	8	O^{2-}	8b	0.0730	0.9750	0.4404	1.00	1.00
O4	8	O^{2-}	8b	0.9600	0.9260	0.3185	1.00	1.00
O5	8	O^{2-}	8b	0.2940	0.2850	0.1215	1.00	1.00
O6	8	O^{2-}	8b	0.1590	0.2000	0.8690	1.00	1.00

Table 2. Parameters of the model structure used for XRD pattern fitting (see Fig. 4).

Space group number	69
Space group	*Fmmm*
Cell choice	1
Lattice parameters	5.4238 Å, 5.3941 Å, 32.9400Å
Angles	90.00°, 90.00°, 90.00°
Atoms in asymmetric unit	9
Atoms in unit cell	76.0, 76 generated position
Volume of the cell	967.92 $Å^3$
Relative mass of unit cell	4686.46
X-ray density	8.0400 g/cm^3
Mass absorption coefficient	287.41 cm^{-1}/g

Name	P. No.	Ion	Wyck.	*x*	*y*	*z*	SOF	B
Bi1	83	Bi3+	8i	0.000	0.000	0.933	1.0	0.00
Bi2	83	Bi3+	8i	0.000	0.000	0.789	1.0	0.00
O1	8	O2-	8e	0.250	0.250	0.000	1.0	0.00
O2	8	O2-	8f	0.250	0.250	0.250	1.0	0.00
O3	8	O2-	8i	0.000	0.000	0.564	1.0	0.00
O4	8	O2-	8i	0.000	0.000	0.692	1.0	0.00
O5	8	O2-	16j	0.250	0.250	0.128	1.0	0.00
Ti1	22	Ti4+	4b	0.000	0.000	0.500	1.00	0.00
Ti2	22	Ti4+	8i	0.000	0.000	0.628	1.00	0.00

Table 3. Details of the calculated X-ray spectrum (see Fig. 3)

Source	X-ray, Co-$K_{\alpha 1+2}$, 1.789007Å, 1.792892Å (α_2/α_1 = 0.497)
2Θ	10.00–72.00°
Geometry	Bragg–Brentano, fixed slit, no anomalous dispersion
Condition	$I \geq 5.00$

hkl	2Θ [deg]	d_{hkl} [Å]	*I* [rel.]	|*F*(*hkl*)|	*Mu*	FWHM
004	12.447	8.25150	6.32	212.07	2	0.4226
006	18.717	5.50100	13.10	463.21	2	0.4316
008	25.043	4.12575	7.84	485.16	2	0.4442
111	27.177	3.80728	26.20	483.32	8	0.4493
117	35.006	2.97418	100.00	1239.75	8	0.4716
020	38.533	2.71090	19.08	1203.63	2	0.4835
200	38.553	2.70959	19.59	1220.35	2	0.4836
0014	44.595	2.35757	12.10	1128.25	2	0.5067
028	46.510	2.26559	10.69	786.51	4	0.5148
208	46.526	2.26483	11.32	809.82	4	0.5149
220	55.648	1.91643	20.14	1323.89	4	0.5585
1115	55.906	1.90829	8.65	616.86	8	0.5599
0214	60.374	1.77895	10.15	1030.01	4	0.5847
2014	60.388	1.77858	10.14	1030.05	4	0.5848
137	67.444	1.61124	16.98	1062.95	8	0.6288
317	67.470	1.61069	16.78	1057.03	8	0.6290

Table 4. Details of the calculated X-ray spectrum (see Fig. 4).

Source	X-ray $Co_{K(1+2)}$, 1.789007Å, 1.792892Å (α_2/α_1 = 0.497)
2Θ	10.000–71.990
Geometry	Bragg–Brentano, fixed slit, no anomalous dispersion
Condition	$I \geq 5.00$

hkl	2Θ [deg]	d_{hkl} [Å]	*I* [rel.]	|*F(hkl)*|	*Mu*	FWHM
004	12.472	8.23500	6.67	215.89	2	0.4941
006	18.754	5.49000	14.32	479.77	2	0.5018
008	25.094	4.11750	8.15	490.06	2	0.5128
111	27.236	3.79912	23.66	455.16	8	0.5172
117	35.082	2.96797	100.00	1228.71	8	0.5368
200	38.519	2.71189	20.31	1227.22	2	0.5470
020	38.739	2.69703	20.10	1228.61	2	0.5477
0014	44.689	2.35286	13.46	1179.69	2	0.5680
208	46.527	2.26480	12.39	837.43	4	0.5750
028	46.716	2.25612	12.32	839.18	4	0.5757
220	55.778	1.91232	24.60	1450.54	4	0.6150
1115	56.030	1.90441	7.55	571.01	8	0.6162
2014	60.440	1.77720	10.57	1040.81	4	0.6386
0214	60.598	1.77300	10.53	1041.89	4	0.6395
317	67.471	1.61066	17.15	1056.69	8	0.6791
137	67.770	1.60442	17.06	1058.57	8	0.6810

The *R*-values of the Rietveld analysis obtained assuming the *B*2*cb* space group are: R_p = 27%, R_{wp} = 42.95%, R_e = 5%, whereas, the *R*-values for the assumed SG *Fmmm* are R_p = 26.82%, R_{wp} = 41.44%, $R_{\exp}$ = 5%. Although the numerical criteria of the goodness of fit (i.e. the *R*-values) are very important, it is necessary to point out that they do not fully reflect the quality of fitting. Graphical criteria such as plots of the calculated and observed intensities and plots of their differences are also necessary. From the traces on the bottom of Figs. 3 and 4, one can see that there are no gross errors of fitting, which might originate in bad scaling parameters, an incorrect crystalline structure used for simulation, or incorrect elementary cell parameters. However, one can see the "negative" lines at the diffraction angle 2Θ = 35.0° and 2Θ = 38.5°. These "negative" lines may arise from the difference between the supposed, pure stoichiometric chemical composition $Bi_4Ti_3O_{12}$ (see Tables 1 and 2, column SOF) and the actual chemical composition of the grown BTO thin film (our BTO films depart by 6% from the theoretical Bi/Ti ratio).

For the films crystallized on Si substrates at 650 °C for 2h, the calculated parameters were (for the expected SG *B*2*cb*): *a* = 5.416(2)Å, *b* = 5.413(2)Å, and *c* = 32.920(0)Å (Table 1), or (for the expected SG *Fmmm*): *a* = 5.423(8)Å, *b* = 5.394(1)Å, and *c* = 32.940(0)Å (Table 2). These parameters slightly differ from the values given in the JCPDS 12-213 data input for the single crystal(*a* = 5.41Å, *b* = 5.45Å and *c* = 32.84Å). These differences may be attributed to the influence of several parameters, such as the substrate, crystallization conditions, grain size, and others. Depending on the substrate and growth conditions, undesired phases such as $Bi_4Ti_8O_{12}$, $Bi_2Ti_2O_7$, or Bi_2O_3 sometimes occur [7]. It is important that for the films studied in this work, only the single phase of $Bi_4Ti_3O_{12}$, grown at 650 °C, was been observed.

The structural determinations presented above prove that the compound crystallizes with the orthorhombic symmetry, as shown in Figs. 3 and 4. On the other hand, the crystallization of BTO thin films in the SG *B*1*a*1 system (ICSD data file 70000 [12]) has not been observed.

4. Conclusions

Randomly oriented $Bi_4Ti_3O_{12}$ thin films were grown on silicon and stainless steel substrates by sol-gel spin coating. Chemical composition microanalyses carried out by EDS showed the following stoichiometric errors: for Ti – 4.6%, for Bi – 1.2%, and for O – 1.8%. It can be concluded that the processing route used for thin film fabrication preserves the stoichiometry (a 6% departure from the theoretical Bi/Ti ratio). X-ray diffraction analysis proved the formation of bismuth layer-structured BTO thin films with orthorhombic structure. Preference is given to the *Fmmm* space group, due to the smaller *R*-values obtained in simulations. No evidence of monoclinic *B*1*a*1 phases was found.

The results of these investigations suggest that our modified sol-gel technique can prevent the formation of cracks and yields dense micro-structured perovskite-type films on metal and single crystal substrates.

References

[1] CZEKAJ D., *Technology Properties and Applications of PZT Thin Films*, Wyd. Uniw. Śl., Katowice, 2002.
[2] SUROWIAK Z., GEGUZINA G., FESENKO E., LISIŃSKA A., SHUVAEVA E., Polish J. Appl. Chem., 38 (1994), 3.
[3] SUBBARAO E.C., Phys.Rev., 122 (1961), 804.
[4] AURIVILLIUS B., Arkiv Kemi, 1 (1950), 499.
[5] CUMMINS S. E., CROSS L. E. J. Appl. Phys., 39 (1968), 2268.
[6] JIN SOO KIM, SANG SU KIM, JONG KUK KIM, TAE KWON SONG, Jpn. J. Appl. Phys., 41 (2002), 6451.
[7] ARAUJO E.B., NUNES V.B., ZANETTE S.I., EIRAS J.A., Mat. Lett.,49 (2001) 108.
[8] KONG L.B., MA J., Thin Solid Films, 379 (2000), 89.
[9] MOROZOV M. I., MEZENTSEVA L. P., GUSAROV V. V., Russian J. Gen. Chem., 72, (2002), 1038.
[10] ARAUJO E. B., EIRAS J. A., J. Eur. Ceram. Soc., 19 (1999), 1453.
[11] SEDLAR M., SAYER M., Ceramics Int., 22 (1996), 241.
[12] RAE A.D., THOMPSON, J.G., WITHERS R.L., WILLIS A.C., Acta Cryst., B46 (1990), 474.
[13] CHU M.-W., CALDES M.T., PIFFARD Y., MARIE A.-M., GAUTIER E., JOUBERT O., GANNE M., BROHAN L., J. Sol. State Chem., 172 (2003), 389.
[14] *The Rietveld Method*, R.A. Young (Ed)., Oxford University Press, Oxford, 1995.
[15] NOLZE G., KRAUS W., *Powder Diffraction*, 13, (1998), 256.
[16] DORRIAN J.I., NEWHAM R.E., SMITH D.K., Ferroelectrics, 3 (1971), 17.

Received 12 August 2004
Revised 8 December 2004